F2008-SC-022

EXTENDED KALMAN FILTERING FOR STATE OF CHARGE ESTIMATION OF LEAD-ACID BATTERIES

[1]Han, Jaehyun*, [2]Sunwoo, Myoungho
[1]Department of Automotive Engineering, Graduate School, Hanyang University, Korea
[2]Department of Automotive Engineering, Hanyang University, Korea

KEYWORDS – lead-acid battery, state of charge (SOC), estimation, Extended Kalman filter (EKF)

ABSTRACT - Lead-acid batteries are widely used in conventional internal combustion engine vehicles, and some electric vehicles. In order to improve the longevity, performance, reliability, density, and economics of batteries, a precise state of charge (SOC) estimation is required. Kalman filtering is one of the techniques used to determine the SOC. For a nonlinear battery model, nonlinear Kaman filters such as an extended Kalman filter and a sigma point Kalman filter are used. However, these nonlinear Kalman filters that are used in other studies are very complicated to apply to lead-acid batteries due to the complex nonlinear model of the battery. In this study, we represent a battery model with simple nonlinear equations, which can represent the battery dynamics for a non-zero battery current. Then, we applied an extended Kalman filter (EKF) method to estimate the SOC of the battery. As a result of that, we proved that the EKF can effectively estimate the SOC using the simple nonlinear battery model.

TECHICAL PAPER

I. INTRODUCTION

Lead-acid batteries, invented in 1859, are the oldest type of rechargeable battery [1]. Lead-acid batteries are still widely used in electrical systems such as conventional internal combustion engine vehicles and some electric vehicles. To improve the longevity, performance, reliability, density, and economics of batteries, an accurate state of charge (SOC) estimation is necessary [3]. For these reasons, several methods for SOC estimation have been developed including coulomb counting, open circuit voltage methods, impedance spectroscopy, electro-motive-force methods, fuzzy logic, and Kalman filters [1]. Among these SOC estimation techniques, a Kalman filter can estimate the SOC dynamically using a battery model [2]. For a nonlinear battery model, nonlinear Kalman filters have been applied such as an extended Kalman filter (EKF) [3-6] and a sigma-point Kalman filter [7, 8].

However, the nonlinear battery models have complex nonlinear equations in SOC estimation methods using the nonlinear Kalman filter [4-8]. For this reason, the SOC estimation algorithm cannot be easily implemented in practice.

In this study, a nonlinear battery model is represented by simple nonlinear equations. This simple nonlinear battery model can effectively show the battery behavior. By using this nonlinear battery model, the SOC of the battery was determined by the EKF with an estimation error of ± 5%. Therefore, the simple nonlinear battery model and the SOC estimation algorithm using the EKF can be implemented in practice.

II. BATTERY MODEL

Battery Model Structure

In order to apply the EKF to the SOC estimation, a nonlinear battery model is required. In this study, the zero-state hysteresis model structure was used for a discrete lead-acid battery model [4, 5]. Equations (1-2) represents the zero-state hysteresis model structure.

$$\begin{aligned} s_{k+1} &= \mathrm{f}(s_k, i_k) + w_k \\ &= s_k - \left(\frac{\eta_i T}{C}\right) i_k + w_k \end{aligned} \tag{1}$$

$$\begin{aligned} y_k &= g(s_k, i_k) + v_k \\ &= \mathrm{OCV}(s_k) + R i_k + h_k H + v_k \end{aligned} \tag{2}$$

Where, s is the SOC state, i is the battery current, y is the battery terminal voltage, R is the battery internal resistance, H is the hysteresis value, and h is a hysteresis constant to represent the sign of the hysteresis effect according to the current. For some ε sufficiently small and positive,

$$h_k = \begin{cases} -\mathrm{sgn}(i_k), & |i_k| > \varepsilon \\ h_{k-1}, & |i_k| \le \varepsilon \end{cases}. \tag{3}$$

In addition, η_i is the columbic efficiency ($\eta_i = 1$ for discharge, and $\eta_i \le 1$ for charge), T is the sampling period, C is the nominal capacity, and w and v are independent, zero-mean, Gaussian noises for process and measurements, respectively. OCV(s_k), the open-circuit voltage as a function of SOC, can be computed as

$$\mathrm{OCV}(s_k) = K_0 + \frac{K_1}{s_k} + K_2 s_k + K_3 \ln(s_k) + K_4 \ln(1 - s_k)\,. \tag{4}$$

Experiments

A lead-acid battery with a nominal voltage of 8 V and a nominal capacity of 100 Ah was tested. For this test, an electronic load was used at room temperature. This electronic load can consume the battery current with an accuracy of ±0.3%. The battery terminal voltage and current were measured by a DAQ system, using Labview® from National Instruments.

The battery was tested on two types of current profile. These current profiles are shown in Fig. 1 and 2. In the each type of current profile, the battery was discharged or charged based on the constant current pulse and rest sequences. For the discharge, the battery was discharged from 100 down to 10 A. For the charge, the battery was charged from 100 down to 10 A. The positive current means the discharge, and the negative current means the charge. According to the discharge and charge current profiles, the battery terminal voltage was decreased and increased, respectively. These battery terminal voltage profiles are shown in Fig. 3 and 4. Furthermore, SOC profiles of battery were obtained by Ah counting method. Figure 5 and 6 show these SOC profiles of battery based on the discharge and charge current profiles.

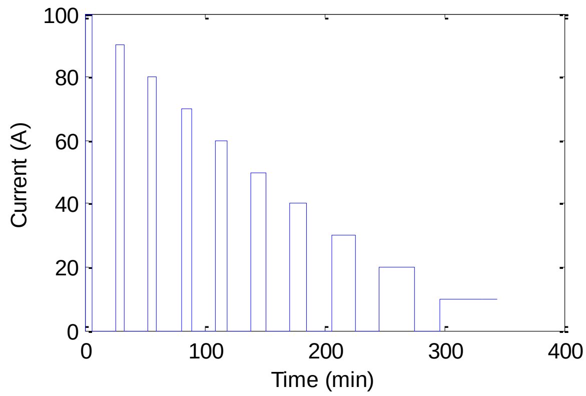

Fig. 1 Discharge current

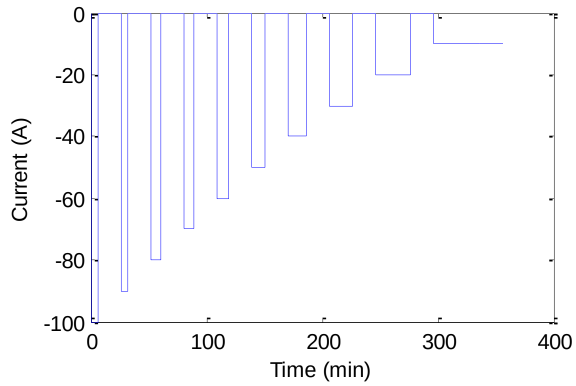

Fig. 2 Charge current

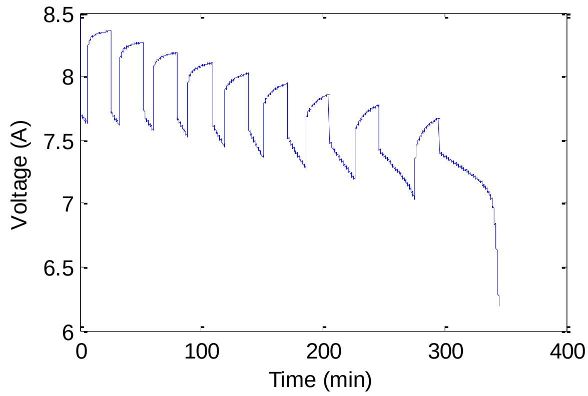

Fig. 3 Discharge voltage

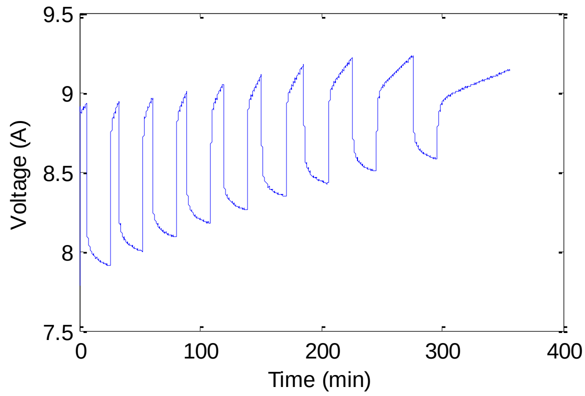

Fig. 4 Charge voltage

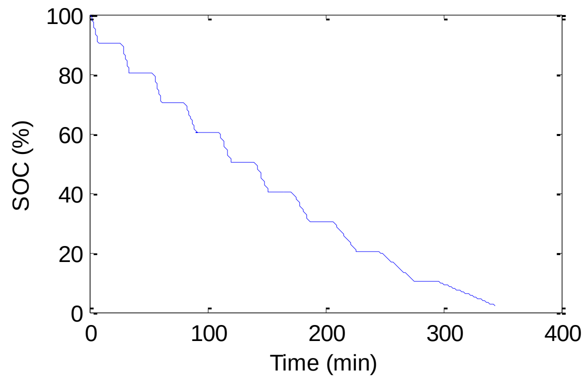

Fig. 5 Discharge SOC

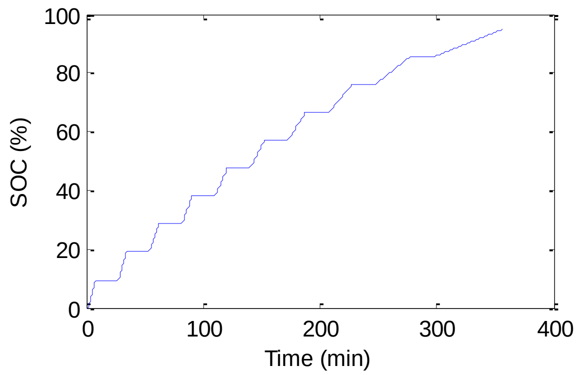

Fig. 6 Charge SOC

Model Parameter Identification

Model parameters were determined by applying the least-square method. For using the least-square method, the battery model output equation can be represented as a regression model as shown in Eq. (5).

$$
\begin{aligned}
y_k &= g(s_k, i_k) \\
&= \mathrm{OCV}(s_k) + Ri_k + h_k H \\
&= K_0 + \frac{K_1}{s_k} + K_2 s_k + K_3 \ln(s_k) + K_4 \ln(1 - s_k) + Ri_k + h_k H \\
&= \begin{bmatrix} 1 & 1/s_k & s_k & \ln(s_k) & \ln(1-s_k) & i_k^+ & i_k^- & h_k \end{bmatrix} \begin{bmatrix} K_0 & K_1 & K_2 & K_3 & K_4 & R^+ & R^- & H \end{bmatrix}^T \\
&= \varphi_k^T \theta
\end{aligned}
\quad (5)
$$

Here, i^+ and i^- are the discharge and charge currents, respectively, where i_k^+ is equal to i_k if $i_k > 0$, i_k^- is equal to i_k if $i_k < 0$. Otherwise, i^+ and i^- are zero. Likewise, R^+ and R^- are the battery internal resistances for discharge and charge, respectively. For N number of observations, Eq. (5) can be written as

$$\mathbf{Y} = \Phi \theta \tag{6}$$

where $Y = [y_1, y_2, \ldots, y_N]^T$ and $\Phi = [\varphi_1^T, \varphi_2^T, \ldots, \varphi_N^T]^T$. As a result, the parameters can be obtained from $\theta = (\Phi^T\Phi)^{-1}\Phi^T Y$ for a non-singular $(\Phi^T\Phi)$. For this determination of parameters, each observation in which the current was not zero was considered, because the zero-state hysteresis model cannot represent the slow variation of the effect of the time constant when the battery current is zero. Table 1 shows the values of the parameters used. For these parameters, the modelling results for discharge and charge are shown in Fig. 7 and 8, respectively. In Fig. 7 and 8, the battery model predicts the battery output voltages with respect to the discharge and charge currents, respectively, whose values are not zero.

Table 1 Battery modelling parameters

K_0	K_1	K_2	K_3	K_4	R^+	R^-	H
6.8143	6.4382×10^{-5}	3.0301	0.045671	0.076233	-2.3626×10^{-2}	-2.5436×10^{-2}	-0.56082

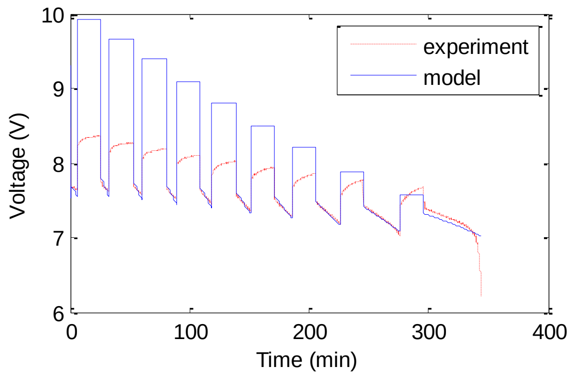

Fig. 7 Modelling result under discharge

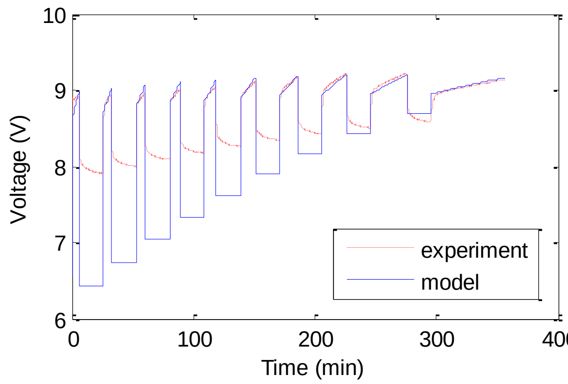

Fig. 8 Modelling result under charge

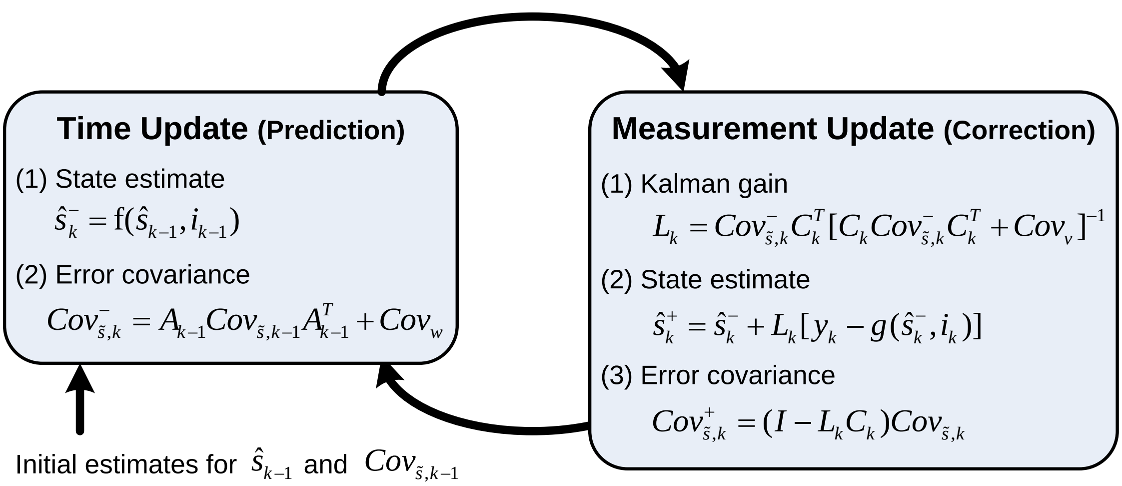

Fig. 9 The operation of the extended Kalman filter

Table 2 EKF time update equations

$\hat{s}_k^- = \mathrm{f}(\hat{s}_{k-1}, i_{k-1})$	(7)
$Cov_{\tilde{s},k}^- = A_{k-1} Cov_{\tilde{s},k-1} A_{k-1}^T + Cov_w$	(8)

Table 3 EKF measurement update equations

$L_k = Cov_{\tilde{s},k}^- C_k^T [C_k Cov_{\tilde{s},k}^- C_k^T + Cov_\upsilon]^{-1}$	(9)
$\hat{s}_k^+ = \hat{s}_k^- + L_k [y_k - g(\hat{s}_k^-, i_k)]$	(10)
$Cov_{\tilde{s},k}^+ = (I - L_k C_k) Cov_{\tilde{s},k}$	(11)

III. SOC ESTIMATION

Extended Kalman Filtering

Kalman filters are widely used in estimation problems [9]. For the nonlinear battery model in this study, the EKF was applied to estimate the SOC of the battery. The operation of the EKF is shown in Fig. 9 [10, 11]. First, the initial state and state error covariance are determined. Then, the state and state error covariance are predicted using the model. After that, the state and error covariance are corrected by using the output measurement. This prediction and correction sequence is repeated at every time step except when the battery current is zero. The equations in the operation of the EKF are shown in Tables 2 and 3 where A_k and C_k are defined by the following equations:

$$A_k = \left. \frac{\partial f(s_k, i_k)}{\partial s_k} \right|_{s_k = \hat{s}_k^+} \qquad (12)$$

$$C_k = \left. \frac{\partial g(s_k, i_k)}{\partial s_k} \right|_{s_k = \hat{s}_k^-} \qquad (13)$$

From the battery model in Eq. (1, 2), the EKF time and measurement update equations can be computed as follows.

$$\hat{s}_k^- = \hat{s}_{k-1} - (\frac{\eta_i T}{C}) i_{k-1} \qquad (14)$$

$$Cov_{\tilde{s},k}^- = Cov_{\tilde{s},k-1} + Cov_w \qquad (15)$$

$$L_k = Cov_{\tilde{s},k}^- C_k^T [C_k Cov_{\tilde{s},k}^- C_k^T + Cov_v]^{-1} \qquad (16)$$

$$C_k = -\frac{K_1}{(\hat{s}_k^-)^2} + K_2 + \frac{K_3}{\hat{s}_k^-} - \frac{K_4}{1 - \hat{s}_k^-} \qquad (17)$$

$$\hat{s}_k^+ = \hat{s}_k^- + L_k [y_k - (K_0 + \frac{K_1}{\hat{s}_k^-} + K_2 \hat{s}_k^- + K_3 \ln(\hat{s}_k^-) + K_4 \ln(1 - \hat{s}_k^-) + R i_k + h_k H)] \qquad (18)$$

$$Cov_{\tilde{s},k}^+ = (I - L_k C_k) Cov_{\tilde{s},k} \qquad (19)$$

SOC Estimation Results

From the experimental data and the EKF model, the SOC of the battery was estimated. In this estimation, the initial values of the state and the state error covariance, the process noise covariance, and the measurement noise covariance used are shown in Table 4. The SOC estimation results are displayed in Figs. 10 and 11. As shown in Figs. 12 and 13, the SOC estimation errors quickly converge into the ± 5% error bound.

Table 4 Simulation condition of the SOC estimation

$\hat{s}_0$	$Cov_{\tilde{s},0}$	Cov_w	Cov_v
50 %	1	1	1

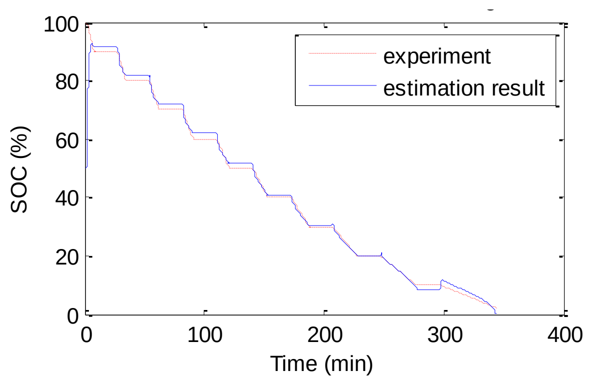

Fig. 10 SOC estimation result under discharge

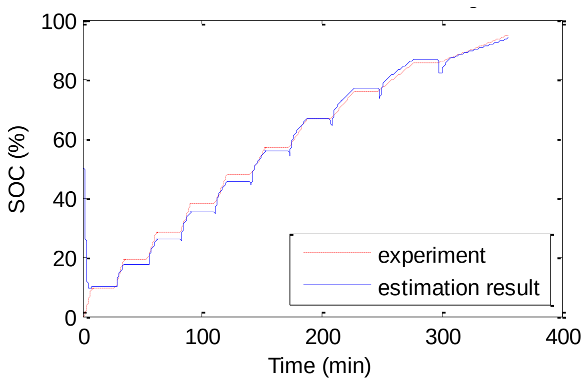

Fig. 11 SOC estimation result under charge

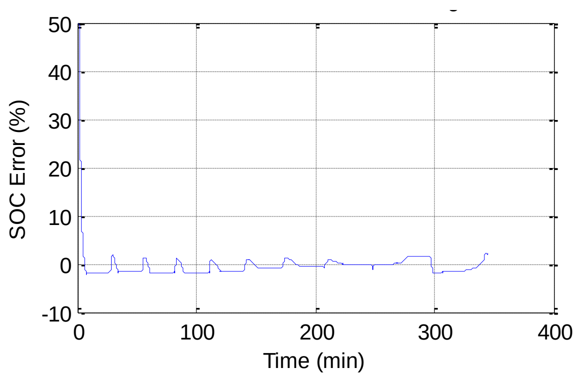

Fig. 12 SOC estimation error under discharge

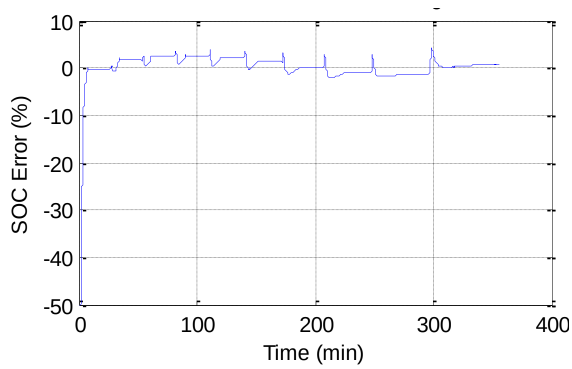

Fig. 13 SOC estimation error under charge

CONCLUSION

In this study, a lead-acid battery was modeled by a simple nonlinear equation. This nonlinear battery model represented the battery output voltage according to the battery current input when the current was not equal to zero. For this simple nonlinear battery model, the SOC of the battery was estimated using the EKF. Consequently, the simple nonlinear battery model and the EKF algorithm, which does not consider zero battery current, can effectively estimate the SOC.

REFERENCES

(1) V. Pop, H.J. Bergveld, P.H.L. Notten, P.P.L. Regtien, “State-of-the-art of battery state-of-charge determination,” Measurement Science and Technology, 16, R93-R110, 2005

(2) S. Piller, M. Perrin, A. Jossen, “Methods for state-of-charge determination and their applications,” Journal of Power Sources, 96, 113-120, 2001

(3) G. L. Plett, “Extended Kalman filtering for battery management systems of LiPB-based HEV battery packs. Part 1. Background,” Journal of Power Sources, 134, 252–261, 2004

(4) G. L. Plett, “Extended Kalman filtering for battery management systems of LiPB-based HEV battery packs. Part 2. Modeling and identification,” Journal of Power Sources, 134, 262–276, 2004

(5) G. L. Plett, “Extended Kalman filtering for battery management systems of LiPB-based HEV battery packs. Part 3. State and parameter estimation,” Journal of Power Sources, 134, 277-292, 2004

(6) A. Vasebi, M. Partovibakhsh, S. M. T. Bathaee, “A novel combined battery model for state-of-charge estimation in lead-acid batteries based on extended Kalman filter for hybrid electric,” Journal of Power Sources, 161, 1369–1384, 2007

(7) G. L. Plett, “Sigma-point Kalman filtering for battery management systems of LiPB-based HEV battery packs. Part 1. Introduction and state estimation,” Journal of Power Sources, 161, 1356–1368, 2006

(8) G. L. Plett, “Sigma-point Kalman filtering for battery management systems of LiPB-based HEV battery packs. Part 2. Simultaneous state and parameter estimation,” Journal of Power Sources, 161, 1369–1384, 2006

(9) R. E. Kalman, “A New Approach to Linear Filtering and Prediction Problems,” Transactions of the ASME, Journal of Basic Engineering, 82 (Series D), 35-45, 1960

(10) M. S. Grewal, A. P. Andrews, “Kalman Filtering: Theory and Practice using MATLAB,” 2nd ed., John Wiley & Sons, 2001

(11) S. Haykin, “Kalman Filtering and Neural Networks,” John Wiley & Sons, 2001